The Journal of Immunology
RESEARCH ARTICLE | DECEMBER 01 2013

Complement Factor B Is the Downstream Effector of TLRs and Plays an Important Role in a Mouse Model of Severe Sepsis FREE

Lin Zou; ... et. al

J Immunol (2013) 191 (11): 5625–5635.
https://doi.org/10.4049/jimmunol.1301903

Complement Factor B Is the Downstream Effector of TLRs and Plays an Important Role in a Mouse Model of Severe Sepsis

Lin Zou,* Yan Feng,* Yan Li,* Ming Zhang,* Chan Chen,* Jiayan Cai,* Yu Gong,* Larry Wang,† Joshua M. Thurman,‡ Xiaobo Wu,§ John P. Atkinson,§ and Wei Chao*

Severe sepsis involves massive activation of the innate immune system and leads to high mortality. Previous studies have demonstrated that various types of TLRs mediate a systemic inflammatory response and contribute to organ injury and mortality in animal models of severe sepsis. However, the downstream mechanisms responsible for TLR-mediated septic injury are poorly understood. In this article, we show that activation of TLR2, TLR3, and TLR4 markedly enhanced complement factor B (cfB) synthesis and release by macrophages and cardiac cells. Polymicrobial sepsis, created by cecal ligation and puncture in a mouse model, augmented cfB levels in the serum, peritoneal cavity, and major organs including the kidney and heart. Cecal ligation and puncture also led to the alternative pathway activation, C3 fragment deposition in the kidney and heart, and cfB-dependent C3dg elevation. Bacteria isolated from septic mice activated the serum alternative pathway via a factor D–dependent manner. MyD88 deletion attenuated cfB/C3 upregulation as well as cleavage induced by polymicrobial infection. Importantly, during sepsis, absence of cfB conferred a protective effect with improved survival and cardiac function and markedly attenuated acute kidney injury. cfB deletion also led to increased neutrophil migratory function during the early phase of sepsis, decreased local and systemic bacterial load, attenuated cytokine production, and reduced neutrophil reactive oxygen species production. Together, our data indicate that cfB acts as a downstream effector of TLR signaling and plays a critical role in the pathogenesis of severe bacterial sepsis. ***The Journal of Immunology*****, 2013, 191: 5625–5635.**

Severe sepsis is defined as systemic inflammatory response syndrome occurring during an infection with at least one acute organ dysfunction (1). Between 1993 and 2003, age-adjusted hospitalization rate for severe sepsis doubled, and age-adjusted population-based mortality rate increased two-thirds in the United States (2). Although the current therapy with fluid resuscitation, antibiotic coverage, and vasopressors offers survival benefit (3), more effective and specific treatment of sepsis is lacking, and mortality remains high (4). Therefore, a better understanding of the molecular pathogenesis of sepsis is clearly needed to develop novel and more effective therapeutic strategies.

*Department of Anesthesia, Critical Care and Pain Medicine, Massachusetts General Hospital, Harvard Medical School, Boston, MA 02114; †Pathology and Laboratory Medicine, Children's Hospital Los Angeles, Los Angeles, CA 90027; ‡Department of Medicine, School of Medicine, University of Colorado Denver, Aurora, CO 80045; and §Department of Medicine, Washington University School of Medicine, St. Louis, MO 63110

Received for publication July 18, 2013. Accepted for publication September 25, 2013.

This work was supported in part by National Institutes of Health Grants R01-GM080906, R01-GM097259, R01-DK076690, and R01-AI041592 and a grant from the International Anesthesia Research Society.

Address correspondence and reprint requests to Dr. Wei Chao, Massachusetts General Hospital and Harvard Medical School, 55 Fruit Street, Boston, MA 02114. E-mail address: wchao@partners.org

The online version of this article contains supplemental material.

Abbreviations used in this article: AKI, acute kidney injury; AP, alternative pathway; cfB, complement factor B; cfD, complement factor D; CLP, cecal ligation and puncture; CR2, complement receptor 2; DCF, dichlorodihydrofluorescein diacetate; KIM-1, kidney injury molecule 1; NGAL, neutrophil gelatinase-associated lipocalin; Poly (I:C), polyinosinic-polycytidylic acid; qRT-PCR, quantitative RT-PCR; ROS, reactive oxygen species; Trif, Toll/IL-1R domain–containing adapter inducing IFN-β; WT, wild-type.

Both TLRs and the complement system are critical parts of innate immunity (5, 6). Although they have been well studied as separate components in the host defense (7), the interplay between the two components under the pathological conditions such as severe polymicrobial sepsis and their possibly intertwined role in sepsis-induced tissue injury and organ failure are poorly understood. TLRs recognize invading pathogens via pattern recognition (8). Previous studies have demonstrated that TLRs mediate a systemic inflammatory response and contribute to high mortality in animal models of polymicrobial sepsis (9–14), but the downstream mechanisms leading to the TLR-mediated septic injury require further study.

There are three separate but convergent pathways of complement activation (i.e., classical, lectin, and alternative pathway [AP]) (7). Complement factor B (cfB) is a necessary component of the AP. Targeted deletion of cfB leads to abrogation of the AP (15). cfB appears to have a property of inducing cell injury. For instance, cfB mediates endotoxin-triggered cardiomyocyte sarcolemmal injury in vitro (16) and ischemia-induced apoptosis in the kidney (17). Emerging preclinical and clinical data suggest the existence of crosstalk between the two innate immune components (18–21) and a possible role for cfB in sepsis (22, 23). For example, complement promotes TLR-induced IL-6 production and Th17 cell differentiation (19). In mouse macrophages (20) and cardiomyocytes (16), cfB is upregulated by LPS-induced TLR4 activation. Patients with severe sepsis have increased cfB mRNA expression in monocytes (22) and activation of the AP (23). However, the mechanisms by which cfB is regulated and its role in the pathogenesis of severe bacterial sepsis and organ injury remain unknown.

In this study, we hypothesized that cfB acts as a downstream effector of TLR signaling and plays a critical role in severe polymicrobial

sepsis. We tested the specific role of TLR signaling in cfB gene and protein expression in immune cells and cardiomyocytes in vitro and in a mouse model of polymicrobial sepsis in vivo. We examined the AP activation during polymicrobial infection. We studied the impact of cfB genetic deletion on sepsis-related mortality and organ injury and explored the putative underlying mechanisms.

Materials and Methods

Animals

Eight- to 12-wk-old sex- and age-matched mice were used for the studies. $TLR4^{-def}$ mice (C57BL/10ScCr), wild-type (WT) control (C57BL/10ScSn) for $TLR4^{-def}$, and C57BL/6J WT mice were purchased from The Jackson Laboratory and housed in a Massachusetts General Hospital animal facility for at least 1 wk before experiments. $TLR2^{-/-}$, Toll/IL-1R domain–containing adapter inducing IFN-β $(Trif)^{-/-}$, $MyD88^{-/-}$, and $cfB^{-/-}$ mice, all in the C57BL/6 background, were previously described (15, 24–26). $MyD88^{-/-}$ mice and WT controls were provided water supplemented with sulfamethoxazole (4 mg/ml) and trimethoprim (0.8 mg/ml). Antibiotics were stopped for at least 2 wk prior to experiments. All animals were housed in pathogen-free, temperature-controlled, and air-conditioned facilities with 12-h/12-h light/dark cycles and fed with the same bacteria-free diet. All animal care and procedures were performed according to the protocols approved by the Subcommittee on Research Animal Care of Massachusetts General Hospital and are in compliance with the "Guide for the Care and Use of Laboratory Animals" published by the National Institutes of Health.

Macrophage and cardiac cell isolation and culture

Macrophages. Bone marrow cells were harvested from mouse tibias and femurs, cultured, and differentiated into macrophages in the presence of M-CSF as described previously (27). Briefly, cells were isolated and resuspended in RPMI 1640 medium supplemented with 10 ng/ml M-CSF, 5% FBS, 10% horse serum, and penicillin (100 U/ml)-streptomycin (100 μg/ml). Three days later, culture media were changed, and macrophages were used for experiments at day 5.

Cardiac myocytes and fibroblasts. Mouse and rat neonatal cardiomyocytes were prepared as described previously with minor modifications (27). Briefly, the hearts were isolated, dissected from major vessels, and cut into appropriate size pieces. Heart tissues were then incubated in ADS buffer ([pH 7.35] 116 mM NaCl, 20 mM HEPES, 0.8 mM Na_2HPO_4, 5.6 mM glucose, 5.4 mM KCl, and 0.8 mM $MgSO_4$) containing 0.3 mg/ml collagenase 2 (Worthington, Lakewood, NJ) and 0.45 mg/ml pancreatin (Sigma-Aldrich, St. Louis, MO) at 37°C for 10–12 min (mouse tissues) or containing 0.4 mg/ml collagenase 2 and 0.6 mg/ml pancreatin at 37°C for 7 min (rat tissues). Cells in suspension were removed, and the remaining myocardial tissues were further incubated with the enzyme buffer five more times until all tissues were digested. Cells in suspension were centrifuged and resuspended in DMEM/Ham's F-12 containing 20% FBS, 4.5% D-glucose, and penicillin/streptomycin. Attached cardiac fibroblasts were removed after plating cells on dishes for 80 min. For cardiac myocyte cultures, plates were precoated with 5 μg/ml fibronectin and 20 μg/ml gelatin (Sigma-Aldrich). Fibroblasts were passaged and plated. Cardiac myocytes and fibroblasts were incubated in a 5% CO_2 incubator at 37°C for 2 d prior to experiments.

RNA extraction and quantitative RT-PCR

Total RNA was extracted using TRIzol reagent (Sigma-Aldrich) and cDNA synthesized by reverse-transcriptase reaction. mRNA was quantified using quantitative RT-PCR (qRT-PCR) as described previously (28). The sequences of all primers used in the study are listed in Supplemental Table I.

cfB and C3 immunoblotting

For tissue samples, animals were euthanized and perfused with 10 ml cold PBS systemically. Hearts were further perfused from aorta to remove coronary blood. All harvested organs were freshly frozen in liquid nitrogen. Tissue powders or cell pellets were suspended in Nonidet P-40 lysis buffer supplemented with complete protease inhibitor cocktails (Roche Diagnostics, Indianapolis, IN). The supernatants from homogenates were quantified for protein concentration by Bradford method. The same amounts of tissue proteins, diluted serum, lavage supernatant, or cell-culture media were fractionated by SDS-PAGE under reducing conditions and blotted with goat anti-human cfB Ab (Complement Technology) or goat anti-mouse C3 Ab (MP Biomedicals). HRP-conjugated donkey anti-goat IgG (Sigma-Aldrich) was used as the second Ab. Bands were visualized using Luminata Forte Western HRP substrate (Millipore, Billerica, MA).

cfB and C3 immunohistochemistry

The hearts and kidneys were fixed with formalin and paraffin-embedded. Tissue cfB and C3/C3 fragment expressions was detected immunohistochemically. The sections were pretreated with enzyme 1 from the Bond Enzyme pretreatment Kit (Leica Microsystems, Buffalo Grove, IL) for 5 min (cfB) or 10 min (C3) and incubated with either anti-cfB Ab (Quidel, San Diego, CA) at a dilution of 1:2000 or anti-C3 Ab (MP Biomedicals, Santa Ana, CA) at a dilution of 1:1600 for 15 min. Signals were detected with the Leica Bond Polymer ReFine Detection KiT DS 9800 (Leica Microsystems). Appropriate positive and negative controls were stained as well.

Mouse model of polymicrobial sepsis

A clinically relevant rodent model of sepsis was created by cecal ligation and puncture (CLP) as has been described previously (10, 28, 29). Briefly, mice were anesthetized with ketamine (100 mg/kg) and xylazine (4 mg/kg). The abdominal cavity was opened in layers. The feces were gently migrated to fill the distal part of the cecum. The cecum was ligated 1.0 cm from the tip. A through-and-through puncture was made with an 18-gauge needle, and a small amount (droplet) of feces was extruded to ensure the patency of the puncture site before returning it back to the abdominal cavity. The sham-operated mice underwent laparotomy but without CLP. The abdominal wall incision was closed in layers. After surgery, prewarmed normal saline (50 ml/kg body weight) was administered s.c. Postoperative pain control was managed with s.c. injection of bupivacaine (3 mg/kg) and buprenorphine (0.1 mg/kg).

Anti-cfB Ab administration

The monoclonal anti-mouse cfB (mAb1379) has been characterized previously (30, 31). Mice were administrated i.p. 1 mg mAb1379 or equal amount of control mouse IgG (Jackson ImmunoResearch Laboratories, West Grove, PA) 1 h before and 12 h after sham or CLP surgeries. Serum or peritoneal lavage was collected for AP activity assay at the designated time points after the procedures. In separate experiments, kidneys were perfused with cold PBS and analyzed for neutrophil gelatinase-associated lipocalin (NGAL) and kidney injury molecule 1 (KIM-1) mRNA expression by qRT-PCR.

Mortality

Mice subjected to CLP were observed every 6 h during the first 2 d and every 12 h thereafter for up to 14 d.

Cardiac function assessment

Cardiac function was assessed in a Langendorff perfusion system as described previously (10).

Flow cytometry analysis of peritoneal neutrophils

$Gr\text{-}1^+$ neutrophils were quantified by flow cytometry (gated on Gr-1 expression) as described previously (28).

Phagocytosis assay

The phagocytic function of $Gr\text{-}1^+$ neutrophils in the peritoneal cavity was analyzed as described previously (28).

Multiplex cytokine immunoassays

Cytokine concentrations of plasma and peritoneal supernatants were determined using a fluorescent bead–based multiplex immunoassay (Luminex, Austin, TX) as previously described (10, 28).

Bacterial clearance determination

Peritoneal and blood bacterial colony counts were determined as previously described (28).

Detection of intracellular reactive oxygen species

For ex vivo studies, peritoneal cells were harvested 12 h after sham or CLP surgeries. Cells (5×10^5) were incubated with 10 μM redox-sensitive dye dichlorodihydrofluorescein diacetate (DCF; Molecular Probes) at 37°C for 30 min and measured in an FITC channel of flow cytometry. Intracellular reactive oxygen species (ROS) was expressed as mean fluorescence intensity as previously described (28). For in vitro studies, peritoneal lavage was harvested after 1.5 ml RPMI 1640 with 0.05% BSA was injected into

the peritoneal space. A total of 5×10^5 bone marrow–derived neutrophils (28) was treated with 100 μl lavage fluid at 37°C for 2.5 h followed by incubation with 10 μM DCF as above.

Complement AP activity assay

AP activity in mouse serum or peritoneal lavage was assayed as described previously with minor modifications (30–32). Briefly, 10 mg zymosan particles (Sigma-Aldrich) in 2 ml 0.15 M NaCl was first activated by boiling for 60 min and then washed twice in PBS. Bacterial colonies were isolated from the blood and peritoneal lavage of CLP mice and cultured in a standard Luria-Bertani medium. The number of bacteria in solution was calculated by OD_{600} reading (OD_{600} of 1.0 = 8×10^8 cells/ml) taken with a spectrophotometer. For each AP activity assay of serum samples, 1×10^7 zymosan particles or bacteria was added to an assay tube in the presence of 10 mM EGTA (to block the classic and lectin complement pathways) and 5 mM $MgCl_2$. Ten microliters mouse serum as described in the text (Fig. 3, Supplemental Fig. 1, Supplemental Fig. 2A) was added, and all samples were brought to 100 μl with Ca^{2+}/Mg^{2+}-free PBS. Assay mixtures were incubated at 37°C for 30 min, and reactions were stopped by placing the tubes on ice. The zymosan particles or bacteria were centrifuged. The supernatants containing particle-free proteins such as cfB, C3, and their cleaved fragments were removed and frozen for later immunoblotting analysis (below). The zymosan and bacteria pellets were used to measure C3 deposition with a flow cytometer (below). For lavage samples (Supplemental Figs. 2B, 3B, 3C), 100 μl lavage supernatant was incubated with 1×10^7 zymosan particles at 37°C for 30 min in a mixture containing 10 μl $cfB^{-/-}$ mouse serum as complement source in the presence of 5 mM of $MgCl_2$ and 10 mM EGTA in Ca^{2+}/Mg^{2+}-free PBS. To quantify the AP activity, C3 deposition on the zymosan or bacteria particles was detected with an FITC-labeled Ab to C3 (MP Biomedicals, Solon, OH) diluted in 1:100, and fluorescence was measured by flow cytometry. Supernatants from the serum AP reaction were also analyzed by immunoblotting to determine the extent of cfB and C3 cleavage. Four microliters supernatant was mixed with sample buffer under reducing conditions, and proteins were separated in 4–12% SDS-PAGE. cfB/cfB fragments and C3/C3 fragments were blotted and detected as described above. Complement factor D (cfD) was blotted with sheep anti-mouse Ab (R&D Systems, Minneapolis, MN).

Caspase-3 activity assay

Twelve hours after surgery, spleens were harvested and immediately frozen in liquid nitrogen. Tissue powder was suspended on ice using lysis buffer provided by caspase-3 fluorescence assay kit (R&D Systems, Minneapolis, MN) as described previously (27). The same amount of protein was assayed for caspase-3 activity.

Statistical analysis

Statistical analysis was performed using GraphPad Prism 5 software (GraphPad Software, Inc.). Unless stated otherwise, the distribution of the continuous variables was expressed as the mean ± SE. Cytokine production was analyzed by Student *t* test. The *p* values of bacterial clearance analysis were applied on the $\log_{10}$ scale and based on the Student *t* test. All other data were analyzed by two-way ANOVA with Bonferroni post hoc tests for statistic significance unless stated otherwise. The null hypothesis was rejected for $p < 0.05$ with the two-tailed test.

Results

TLRs specifically mediate cfB production in immune and cardiac cells

Pam3Cys (a TLR2 ligand) and LPS (a TLR4 ligand) induced a marked induction of cfB mRNA expression in WT bone marrow–derived macrophages (Fig. 1A). Absence of TLR2 abolished the effect of Pam3Cys, whereas TLR4 deficiency blocked that of LPS. MyD88 deletion completely blocked Pam3Cys-induced cfB expression and partially LPS's effect. Trif deficiency partially blocked LPS's effect and had no effect on TLR2-induced cfB expression (Fig. 1A). Both TLR2 and TLR4 ligands also induced cfB protein expression in macrophages (Fig. 1B). Although serum complement is mainly produced in liver (33), prior studies have suggested that other parenchymal tissues, such as the kidney or heart, or myeloid cells locally produce components that may play a prominent role in renal and cardiac injury (16, 17, 34, 35) or in host defense against pathogen (36), respectively. To test the ability of TLR ligands to induce cfB expression in cardiac cells, we treated cardiomyocytes isolated from WT, $TLR2^{-/-}$, and $TLR4^{-def}$ mice with Pam3Cys or LPS. Similar to macrophages, both Pam3Cys and LPS led to a robust increase in cfB and a relatively modest increase in C3 gene expression, but had no effect on C4 and C5 expression (Fig. 1C). TLR2 or TLR4 deficiency, respectively, completely blocked Pam3Cys- or LPS-induced cfB and C3 gene expression in cardiomyocytes (Fig. 1C). Moreover, stimulation of TLR2 (Pam3Cys), TLR3 (polyinosinic-polycytidylic acid [Poly (I:C)]), or TLR4 (LPS), but not TLR9 (CpG), induced a marked increase in cfB gene (Fig. 1D) and protein expression in rat cardiomyocytes and cardiac fibroblasts (Fig. 1E). Importantly, both cardiomyocytes and cardiac fibroblasts also released a significant amount of cfB into the culture media (Fig. 1E). Together, these data suggest that signaling via different TLRs, including those of TLR2, TLR3, and TLR4, specifically induced marked cfB production in three distinct types of cells (i.e., macrophages, cardiomyocytes, and cardiac fibroblasts).

cfB is upregulated during polymicrobial sepsis

We used CLP as the clinically relevant model of polymicrobial sepsis. We examined organs and found that, at baseline, the liver had the highest and the heart the lowest cfB gene expression (data not shown). However, 24 h after CLP, the heart had the most robust cfB mRNA response (21-fold) compared with the other organs examined (Fig. 2A), whereas the kidney had the most increase in C3 (7-fold) and the liver in C5 (8-fold) gene expression. Importantly, immunoblotting demonstrated that CLP induced a time-dependent upregulation of cfB protein in the heart, lung, kidney, liver, and spleen (Fig. 2B). Immunohistochemistry analysis demonstrated a basal level of cfB in the kidney of the sham mice, particularly in the tubular cells of the cortex, but very little in the heart. Two days after CLP, there was a marked increase in cfB protein localized in the heart and in renal tubular cells in cortex as well as in medulla as compared with that of sham or $cfB^{-/-}$ mice (Fig. 2C). To determine the role of TLR signaling in the sepsis-induced cfB expression, WT, $TLR2^{-/-}$, $TLR4^{-def}$, $MyD88^{-/-}$, and $Trif^{-/-}$ mice were subjected to sham or CLP surgery. In the heart, whereas CLP induced a marked increase in cfB gene expression, there was no difference between WT and mice deficient in TLR2, TLR4, or Trif (Fig. 2D). However, absence of MyD88 led to a significant attenuation in cardiac cfB gene and protein expression following CLP (Fig. 2D, 2E). Taken together, these data suggest that polymicrobial sepsis increases tissue cfB levels in the heart and kidney, and that, at least in the heart, the sepsis-induced cfB production is partially mediated through a MyD88-dependent mechanism.

Polymicrobial sepsis leads to AP activation

Twenty-four and 48 h after CLP procedure, there was an increase in cfB and Ba fragments in both serum and peritoneal lavage samples in WT but not in $cfB^{-/-}$ mice (Fig. 3A), indicating enhanced AP activity during sepsis. To investigate the mechanism by which polymicrobial infection induces AP activation, we tested the role of cfD in serum AP activation induced by pathogens in an in vitro system. In the presence of Mg^{2+} and EGTA (to block classic and lectin pathways), zymosan or bacteria isolated from the blood and peritoneal lavage of septic mice led to robust AP activation in WT serum as demonstrated by cfB and C3 cleavage (Fig. 3B) and marked C3 deposition on zyomsan or bacteria, respectively (Fig. 3C, 3D). cfD deletion (Supplemental Fig. 1A) completely blocked both zymosan- and bacteria-induced AP activation (Fig. 3B–D), suggesting the essential role of cfD in the AP activation during sepsis. Moreover, to further determine the role of TLR signaling in the sepsis-induced AP activation, we tested the impact of MyD88

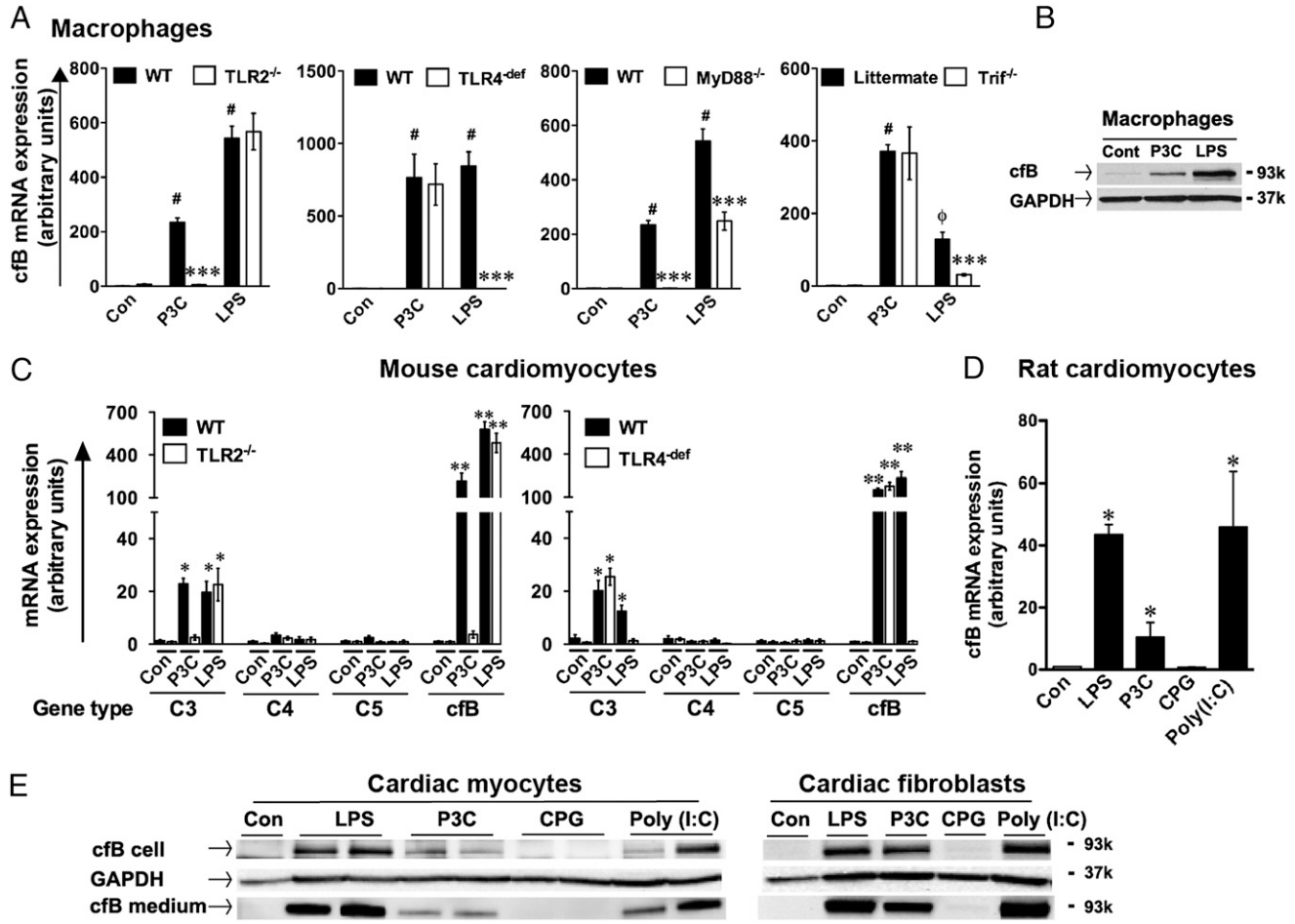

FIGURE 1. Multiple TLR ligands induce a robust cfB production in both macrophages and cardiac cells. (**A**) TLR2 and TLR4 stimulation leads to cfB expression in bone marrow–derived macrophages. Bone marrow–derived macrophages were stimulated by Pam3Cys (P3C; 1 μg/ml) or LPS (500 ng/ml) for 20 or 12 h, respectively. cfB mRNA was measured by qRT-PCR. $n = 4$–6 samples/group. $^{\#}p < 0.001$, $^{\Phi}p < 0.05$ versus the control, $^{***}p < 0.001$ versus WT-LPS. Con, control (normal saline). (**B**) Immunoblotting of cfB in macrophages. Macrophages were stimulated with P3C or LPS. Twenty or 12 h after treatment, cfB was detected by immunoblotting. GAPDH was employed as the internal control to monitor equal protein loading. (**C**) TLR2 or TLR4 stimulation selectively upregulated cfB and C3 gene expression in cardiomyocytes. Mouse neonatal cardiomyocytes isolated from WT, TLR2$^{-/-}$, or TLR4^{-def} mice were stimulated with P3C or LPS for 24 h. C3, C4, C5, and cfB mRNA were measured by qRT-PCR. $n = 4$ in control group, $n = 4$ to 5 in the P3C-treated group, and $n = 3$–5 in the LPS-treated group. $^{*}p < 0.05$, $^{**}p < 0.01$ versus control. (**D**) TLR2–4 ligands induces cfB mRNA expression in rat cardiomyocytes. Rat neonatal cardiomyocytes were stimulated with LPS (500 ng/ml), P3C (1 μg/ml), CpG (CPG; 0.25 μM), and Poly (I:C) (25 μg/ml) for 24 h. cfB mRNA was detected by qRT-PCR. $n = 3$ in each group. $^{*}p < 0.05$ versus control group (Con). (**E**) Immunoblotting of cfB: rat neonatal cardiomyocytes and cardiac fibroblasts were stimulated with LPS (500 ng/ml), P3C (1 μg/ml), CpG (0.25 μg/ml), and Poly (I:C) (25 μg/ml) for 24 h. Cells and media were separated, and proteins were immunoblotted for cfB. All experiments were performed at least three times. Con, control.

on serum cfB and C3 expression in sham and septic mice. As shown in Fig. 3E, 48 h after CLP, there was an increase in serum cfB and C3 levels in WT mice. Ba and C3α fragments were also increased. MyD88 deletion almost blocked the sepsis-induced cfB/C3 upregulation and somewhat attenuated cfB/C3 cleavage in vivo. These data suggest that signaling via MyD88 plays an important role in mediating the enhanced cfB/C3 expression and thus AP activation during polymicrobial sepsis in vivo. Of note, in vitro, sera from WT, MyD88$^{-/-}$, and Trif$^{-/-}$ exhibited the same levels of AP activity upon zymosan or bacteria treatment as demonstrated by the same levels of Ba and cleaved C3α (Supplemental Fig. 1B). This suggests that MyD88 is probably not involved in the pathogen-induced cfB/C3 cleavage per se.

cfB$^{-/-}$ mice have reduced C3 cleavage and tissue deposition in the kidney

All three complement pathways converge at C3. C3 is composed of an α- and a β-chain. The α-chain is cleaved by each respective C3 convertase to form C3b, which is further cleaved to C3dg (37). As shown in Fig. 4A, polymicrobial sepsis induced a marked increase in C3 and C3α cleavage fragments in serum and peritoneal lavage fluids, pointing to a systemic C3 upregulation and activation during polymicrobial sepsis. Importantly, whereas absence of cfB had no effect on C3 expression, it nearly abolished C3dg production at 24 and 48 h after CLP procedure (Fig. 4A). These data suggest that cfB and the AP are essential for C3 activation during polymicrobial sepsis in vivo. Moreover, polymicrobial infection also induced a time-dependent increase in C3 mRNA expression in the kidney. Consistent with the serum C3 protein levels, cfB deletion has no impact on the C3 mRNA expression (Fig. 4B). Immunohistochemistry study indicated that C3 and C3 fragments were primarily localized in the basal membrane of the cortex as well as in medullary regions of the kidney. cfB$^{-/-}$ mice appeared to have a slightly reduced staining for C3 than WT mice. CLP induced a marked increase in the C3 deposition in the cortex and interstitial localization in the medulla. In comparison, there was a marked reduction in C3/C3 fragment deposition in cfB$^{-/-}$ septic mice, particularly in the noncortex region. These data suggest that

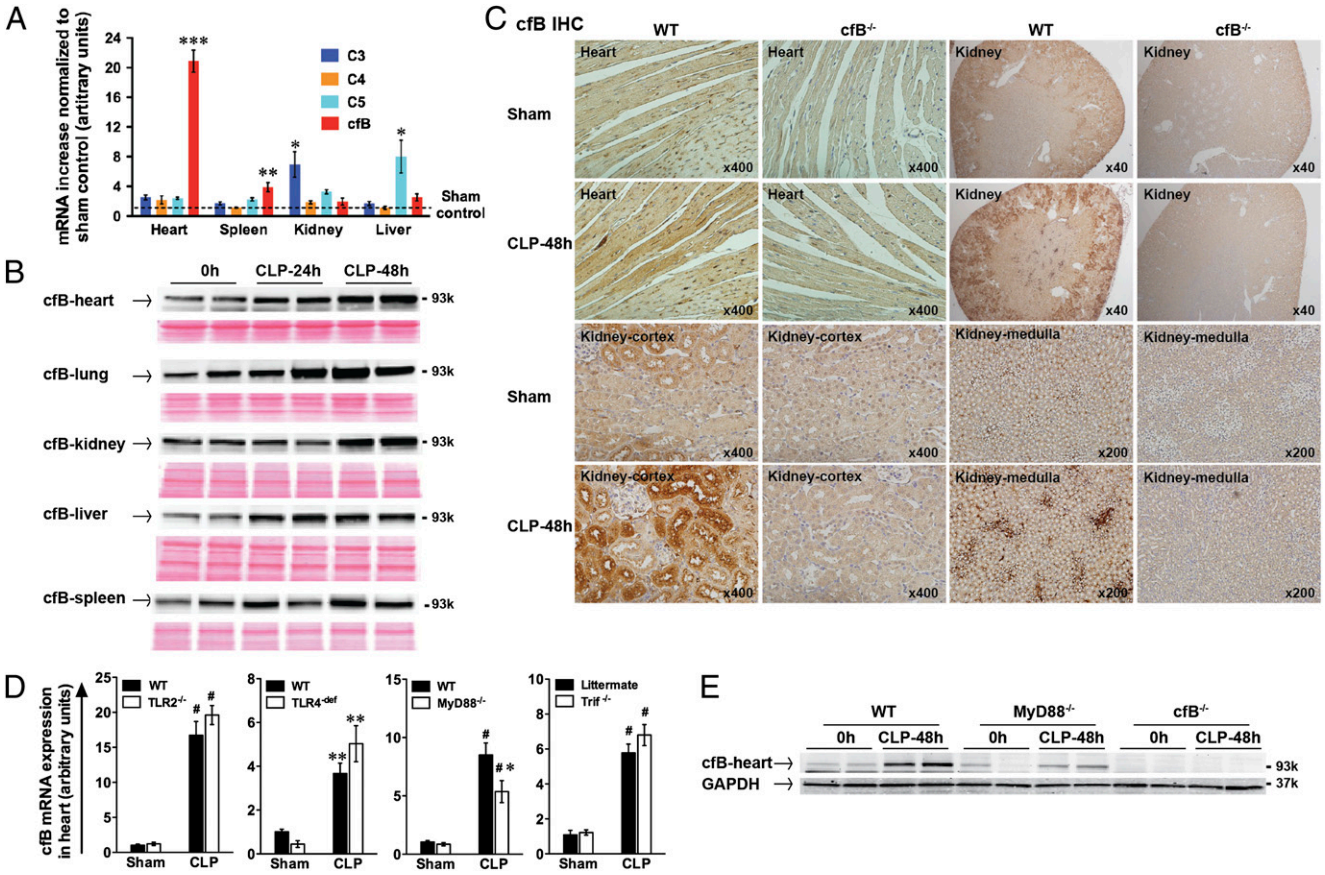

FIGURE 2. Polymicrobial infection induces cfB upregulation. (**A**) qRT-PCR analysis of complement factors in various organs. Mice were subjected to sham or CLP surgery. Twenty-four hours later, C3, C4, C5, and cfB mRNA levels were measured in the heart, spleen, kidney, and liver by qRT-PCR. The arbitrary unit indicates the relative increase of mRNA expression compared with the sham control. $n = 7$ mice/group. $^{*}p < 0.05$, $^{**}p < 0.01$, $^{***}p < 0.001$ versus the sham control. (**B**) Immunoblotting of cfB. Heart, lung, kidney, liver, and spleen were harvested at 0, 24, and 48 h after CLP surgery. cfB protein was detected by immunoblotting. Ponceau protein staining was employed to monitor equal sample loading. (**C**) Immunohistochemistry (IHC) of cfB. Mice were subjected to sham or CLP procedures. Forty-eight hours after the surgery, hearts and kidneys were harvested and sectioned, and immunohistochemistry for cfB was performed. Original magnification: heart section, ×400; kidney section, ×40, ×200, and ×400. (**D**) qRT-PCR analysis of cfB mRNA in the heart. WT, TLR2$^{-/-}$, TLR4$^{-\text{def}}$, MyD88$^{-/-}$, and Trif$^{-/-}$ mice were subjected to sham or CLP surgery. Twenty-four hours later, the hearts were collected, and cfB mRNA was measured using qRT-PCR. $n = 3$–5 mice in sham group, $n = 4$–10 mice in CLP group. $^{*}p < 0.05$ versus WT-CLP, $^{**}p < 0\ 0.01$, $^{\#}p < 0.001$ versus the sham control. (**E**) Immunoblotting of cfB in cardiac tissue. WT, MyD88$^{-/-}$, and cfB$^{-/-}$ mice were subjected to CLP procedure. Forty-eight hours after CLP, the hearts were isolated and the coronary artery perfused with PBS via the aorta. cfB protein was detected by immunoblotting.

cfB mainly affects C3/C3 fragment deposition in the kidney but has no effect on the local kidney C3 synthesis, as cfB deficiency exhibited minimal effect on C3 mRNA in the septic kidney. Similarly, there was a marked increase in C3 deposition 48 h after CLP in the heart, but the increased C3 deposition in the heart appeared to be cfB-independent, as there was no apparent difference between WT and cfB$^{-/-}$ septic hearts (Fig. 4C).

Absence of cfB reduces organ injury and improves survival in sepsis

WT septic mice exhibited a mortality rate of 68% by 14 d. In comparison, cfB$^{-/-}$ septic mice had a significantly lower mortality rate of 42% ($p = 0.02$) (Fig. 5A). Given the significant cfB expression/deposition in the heart and kidney during sepsis, we tested the impact of cfB deficiency on heart dysfunction and acute kidney injury (AKI) in septic mice. As shown in Fig. 5B, WT septic mice developed a severe cardiac dysfunction compared with the sham mice as demonstrated by reduced left ventricular developed pressure, dP/dt_{max}, and dP/dt_{min} (maximal and minimal first derivation of left ventricular developed pressure, respectively), as measured in a Langendorff perfusion system. In comparison, cfB$^{-/-}$ mice had significantly improved cardiac function. AKI is a frequent complication of septic patients in the intensive care unit and associated with a high mortality (38). As illustrated in Fig. 5C, periodic acid-Schiff staining of mouse kidney cortex showed pink brush border in cortical tubules of sham mice and loss of brush border and prominent vacuolization in many tubules of septic mice as previously described (39, 40). In comparison, most brush boarders were preserved and much less tubular vacuolization was seen in the kidney of CLP cfB$^{-/-}$ mice (Fig. 5C). Moreover, the standard blood chemistry such as blood urea nitrogen and creatinine used clinically are much less sensitive than the two recently developed biomarkers, kidney NGAL and KIM-1 (41, 42, 43) for AKI diagnosis during sepsis (39, 40), which reportedly are sensitive indices in the prediction and early diagnosis of AKI (39, 40, 43, 44). As shown in Fig. 5D, NGAL and KIM-1 mRNA levels in the kidney were markedly increased in WT septic mice compared with the sham control. In comparison, cfB$^{-/-}$ mice exhibited significantly attenuated NGAL and KIM-1 mRNA levels in the kidney. Moreover, we administered mice with control IgG or mAb1379, an inhibitory mAb specific for mouse cfB (30). The efficacy of mAb1379 administered 1 h prior to CLP procedure

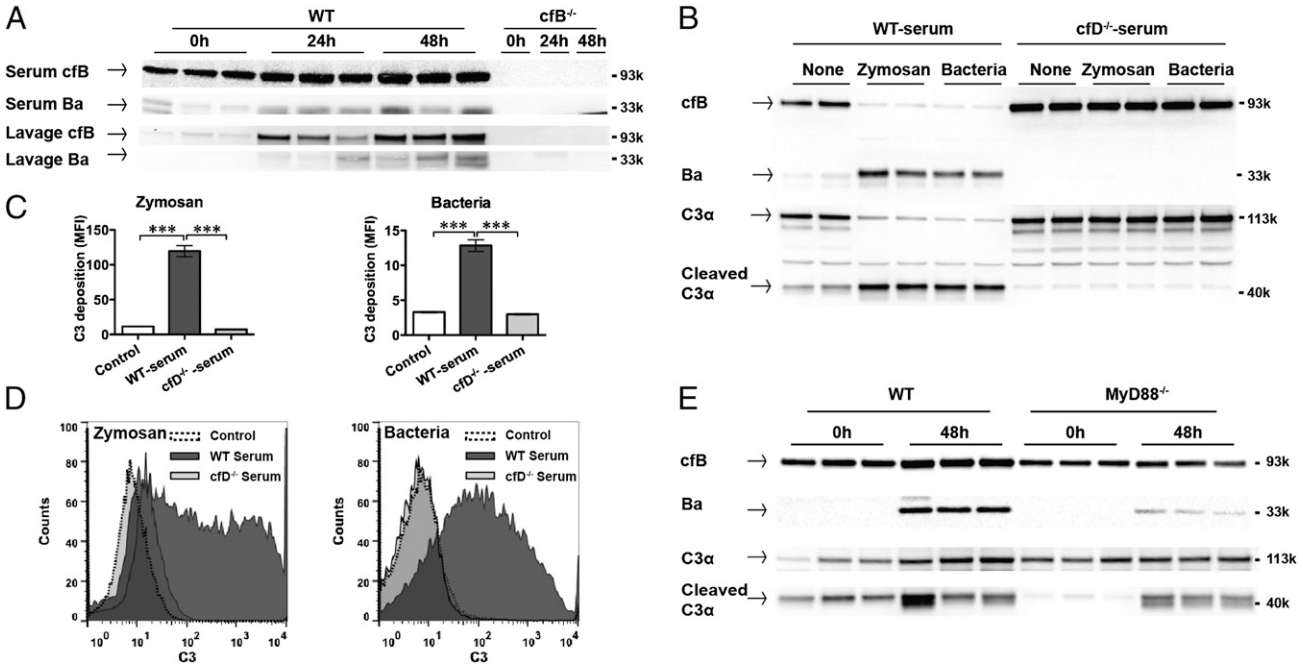

FIGURE 3. Polymicrobial infection induces cfB upregulation and AP activation via a MyD88-dependent mechanism. (**A**) Immunoblotting of cfB and Ba. Mice were subjected to CLP procedure. At 0, 24, and 48 h after CLP, 0.5 ml of lavage fluid was collected after 1.0 ml of normal saline i.p. injection. Blood was collected by cardiac puncture. Total of 40 μl of lavage supernatant and diluted serum (1:100 dilution with Nonidet P-40 lysis buffer) was loaded, and proteins were separated in 4–20% SDS-PAGE. cfB (93 kDa) and Ba fragments (33 kDa) were detected by immunoblotting. $cfB^{-/-}$ mice were used as the negative control. (**B**) Zymosan and bacteria induce serum cfB/C3 cleavage role for cfD. Total of 10 μl of serum from WT or $cfD^{-/-}$ mice was incubated in the presence of Mg^{2+}/EGTA with 1×10^7 zymosan or bacteria isolated from septic mice at 37°C for 30 min. Proteins in supernatants separated in 4–12% SDS-PAGE and immunoblotted for cfB/C3 and their cleaved fragments including Ba, C3α-chain (113 kDa), and cleaved C3α fragments (40 kDa). The pellets containing zymosan or bacteria were used for measuring C3 deposition as described below. (**C**) Zymosan or bacteria induces serum AP activation role of cfD. As noted in (B), AP activation induced by zymosan or bacteria was assessed by measuring C3 deposition on zymosan or bacteria using flow cytometry as described in *Materials and Methods*. The negative control contains no serum. $n = 3$. $^{***}p < 0.001$. (**D**) Representative FACS histograms of AP activation by zymosan or bacteria. (**E**) MyD88 deletion attenuates serum cfB/C3 upregulation and cleavage during polymicrobial infection. WT or $MyD88^{-/-}$ mice were subjected to CLP procedure. At 0 and 48 h after surgery, animals were euthanized, and sera were examined for cfB/C3 and their cleaved fragments as described in *Materials and Methods*.

was evident as serum of mAb1379-treated, but not control IgG-treated, mice completely inhibited AP activation in an in vitro zymosan-based AP assay (Supplemental Fig. 2A). mAb1379 also inhibited AP activity in vitro when incubated with peritoneal lavage fluid to a similar level as $cfB^{-/-}$ mice (Supplemental Fig. 2B). When given 1 h before and again 12 h after surgery, mAb1379-treated mice had significantly lower kidney NGAL and KIM-1 gene expression compared with that of control IgG (Fig. 5E) at both 12 and 24 h after CLP. Taken together, these data demonstrate that cfB contributes to sepsis-induced cardiac dysfunction and AKI.

Neutrophil migration, bacterial clearance, and cytokine storm

There was a marked time-dependent increase in the number of cells migrating into the peritoneal cavity with the peak reached at 24 h following CLP (Fig. 6A). Both the percentage (Fig. 6B) and total number (Fig. 6C) of $Gr\text{-}1^+$ neutrophils in the peritoneal cavity peaked at 24 h after CLP. Importantly, cfB deletion led to an enhanced neutrophil migration during the first 12 h postinfection compared with WT mice ($p < 0.05$) but the difference disappeared at 24 and 34 h (Fig. 6A, 6C). Of note, both WT and $cfB^{-/-}$ mice had markedly increased but the same percentage of $Gr\text{-}1^+$ neutrophils in the peritoneal cavity with the peak at 24 h (Fig. 6B). These data suggest that cfB may contribute to sepsis by attenuating the early neutrophil migratory activity. Moreover, following peritoneal infection, WT peritoneal neutrophils displayed a time-dependent increase in their phagocytic function compared with the neutrophils isolated before the infection (Fig. 6D). However, deletion of cfB had no impact on the phagocytic function of neutrophils. Bacterial load reflects host overall defense ability against bacterial infection. Consistent with the enhanced neutrophil migratory function, $cfB^{-/-}$ septic mice showed a substantially reduced bacterial load in the lavage and blood compared with WT (Fig. 6E). Proinflammatory cytokines are known to contribute to lethality during severe sepsis (45). As illustrated in Fig. 6F, $cfB^{-/-}$ septic mice had decreased IL-6 and TNF-α in both the plasma and local lavage compared with WT septic mice. Plasma IL-10 and keratinocyte chemoattractant were also found significantly lower in $cfB^{-/-}$ septic mice. Finally, lymphocyte apoptosis reportedly plays an important role in the pathogenesis of sepsis and contributes to its mortality (46). As shown in Supplemental Fig. 3A, CLP induced a marked increase in caspase-3 activity in spleen lymphocytes of WT mice, but cfB deficiency had no impact on caspase-3 activation.

Reduced neutrophil reactive oxygen species generation in $cfB^{-/-}$ mice

ROS, especially intracellularly, plays an important role in regulating cytokine production (47, 48) and is associated with organ injury during sepsis (48, 49). ROS generation was assessed using redox-sensitive dye DCF by flow cytometry. As illustrated in Fig. 6G, there was a robust increase in the intracellular ROS in neutrophils of WT septic mice. In comparison, $cfB^{-/-}$ septic mice had a marked reduction in neutrophil ROS production. When WT

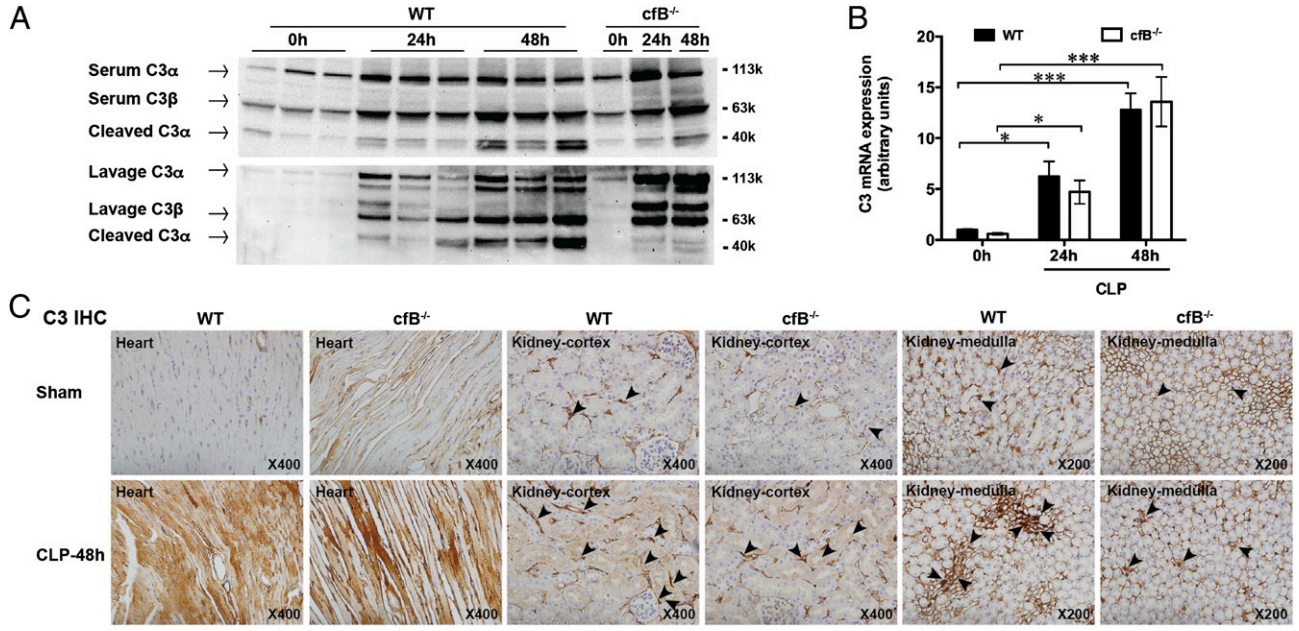

FIGURE 4. cfB deletion attenuates C3 cleavage and tissue deposition in the kidney. (**A**) Immunoblots of serum C3 and C3 fragments. Mice were subjected to CLP procedure. Control mice received no surgery. At 0, 24, and 48 h after CLP, sera were collected and immunoblotted with a C3 Ab that recognizes C3 (both C3α and C3β-chains) and cleaved C3α fragment (known as C3dg). (**B**) C3 mRNA in the kidney before and after CLP. WT and cfB$^{-/-}$ mice were subjected to CLP. At 0, 24, and 48 h after CLP, kidney tissues were collected and analyzed for C3 mRNA expression by qRT-PCR. $n = 3$–7. $^{*}p < 0.05$, $^{***}p < 0.001$. (**C**) Immunohistochemistry (IHC) of C3 and the C3 fragments in the heart and kidney. WT and cfB$^{-/-}$ mice were subjected to sham or CLP procedure. Forty-eight hours after the surgery, the heart and kidney were collected. The tissues were fixed with formalin, paraffin-embedded, and sectioned. C3 and C3 fragments in the heart and kidney were detected immunohistochemically using a specific anti-C3 Ab that recognizes C3 (both C3α and C3β-chains) and cleaved C3α fragment (known as C3dg). The arrowheads point to deposited C3and C3 fragments in the kidney. Original magnification: heart section, ×400; kidney section, ×200 and ×400.

and cfB$^{-/-}$ bone marrow neutrophils were treated with peritoneal lavage in vitro, there was a marked increase in ROS production in both groups of the cells treated with septic lavage compared with that of sham control lavage. Absence of cfB in neutrophils did not affect their ability to generate ROS in response to the lavage treatment (Supplemental Fig. 3B). However, if WT neutrophils were treated with peritoneal lavage from septic WT or cfB$^{-/-}$ mice, there was a trend toward septic WT lavage-treated cells generating more ROS than those treated with septic cfB$^{-/-}$ lavage, but the difference did not reach statistical significance (Supplemental Fig. 3c). Together, the above data suggest that: 1) cfB mediates ROS production in the peritoneal neutrophils in vivo during polymicrobial sepsis, a property also reported for TLR2 signaling (28); 2) the peritoneal lavage fluid from septic mice is sufficient to induce neutrophil ROS production in vitro; and 3) cfB in neutrophils is probably not involved in modulating cellular ROS production during sepsis.

Discussion

The current study made four major observations. First, we show that distinct types of TLRs, including those for Gram-positive and -negative bacteria and for viral RNA, are able to induce a robust cfB production in three different cell types; namely, macrophages, cardiac fibroblasts, and cardiomyocytes. These cells not only undergo de novo synthesis of cfB in response to TLR activation but also release it into the extracellular space. The TLR effect appears relatively specific toward cfB as expression of C4 and C5 is not altered. Second, in a clinically relevant in vivo model of polymicrobial sepsis, which likely involves activation of multiple different types of TLRs, cfB is produced and AP activated via a MyD88-dependent mechanism. Consistent with the widespread cfB upregulation in septic animals, the complement AP is activated both locally and systemically in septic animals and probably via a cfD-dependent mechanism. cfB appears particularly essential for the production of C3-cleaved fragment (i.e., C3dg), a major complement fragment observed in tissue injury (50). Third, absence of cfB confers a survival benefit with a 38% reduction in mortality rate consistent with improvements in heart function and a marked reduction in AKI as evidenced by better preserved left ventricular function and reduced AKI biomarkers. Fourth, we demonstrate that cfB deletion is associated with enhanced early neutrophil migration to the infectious site, less C3 fragment deposition in the kidney, reduced inflammatory cytokine production, decreased bacterial load, and attenuated ROS generation in neutrophils. Taken together, these data suggest that cfB acts as the downstream effector of TLR signaling and plays a pivotal role in the pathogenesis of polymicrobial sepsis.

Our studies demonstrate that distinct types of TLRs are able to induce cfB expression not only in immune cells (macrophages) but also in cardiac fibroblasts and cardiomyocytes, an unusual function for cardiac cells. At least in the case of TLR2 and TLR4 and in cardiomyocytes, the TLR's effect is fairly specific for cfB and C3 as only cfB and C3, but not C4 and C5, gene expression is upregulated. These data are consistent with a previous report in macrophages, indicating that out of 18 complement factors tested, cfB is specifically augmented by TLR4 stimulation (20). Crosstalk between complement system and TLRs appears bidirectional (21). Complement system can also synergistically enhance TLR-induced proinflammatory responses via C3aR- and C5aR-dependent mechanisms in vitro and in vivo (18). Given the important role of these TLRs in the pathogenesis of sepsis (9–14), we hypothesized cfB as a key downstream effector of TLR signaling during sepsis. In a clinically relevant mouse model of polymicrobial sepsis, we demonstrate that sepsis induced a widespread

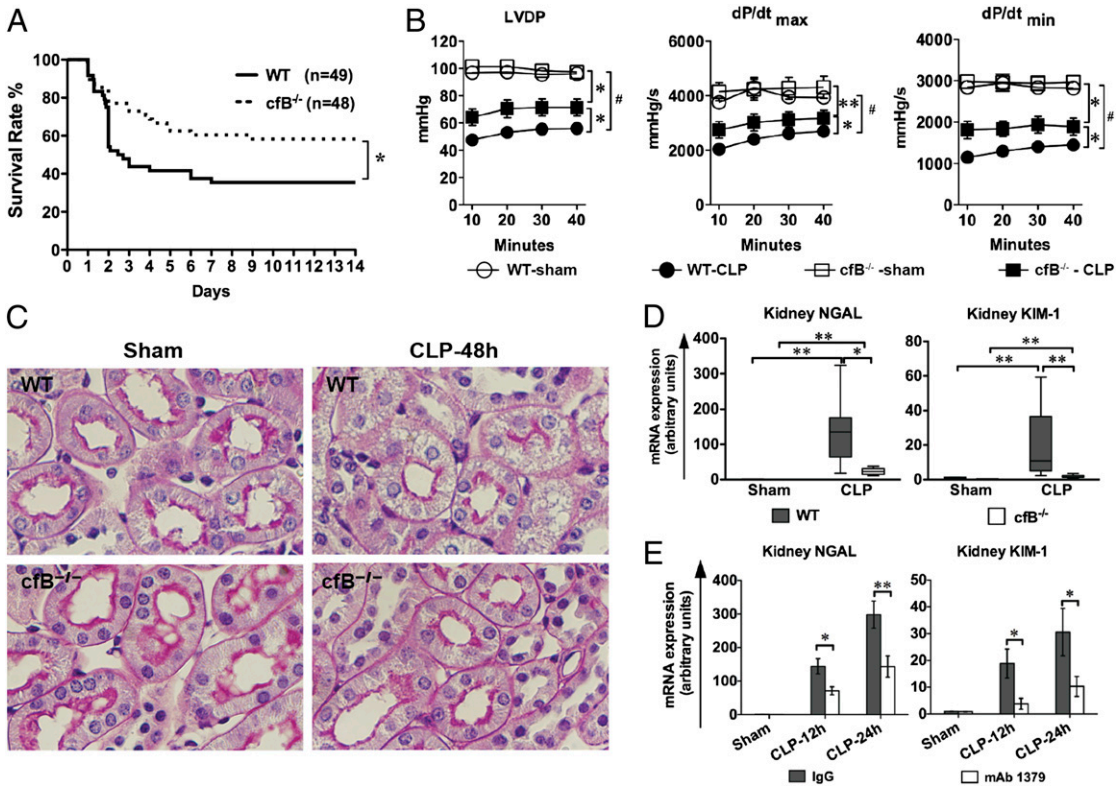

FIGURE 5. Absence of cfB improves survival and reduces organ injury during experimental polymicrobial sepsis. (**A**) Survival rate of WT and cfB$^{-/-}$ mice during sepsis. Mice were subjected to CLP surgery and monitored for survival for up to 14 d. The survival curve includes data from five separate experiments. *$p < 0.05$, 24 h after surgery. (**B**) Cardiac function of the Langendorff perfused heart. Both WT and cfB$^{-/-}$ were subjected to sham and CLP surgeries. Twenty-four hours later, the mice were euthanized and the hearts isolated and perfused at a constant pressure in a Langendorff perfusion system for up to 40 min. Left ventricular developed pressure (LVDP), dP/dt_{max}, and dP/dt_{min} (maximal and minimal first derivation of LVDP, respectively) were recorded as described previously (10, 28). $n = 3$ in sham group, $n = 8$–10 in CLP group. *$p < 0.05$, **$p < 0.01$, $^{\#}p < 0.001$ versus WT-CLP. (**C**) Histology of AKI in CLP-induced sepsis. Periodic acid-Schiff staining of mouse kidney cortex 48 h after sham or CLP surgery. Loss of pink brushboarder and prominent vasculization in most of cortical tubules were observed in CLP WT but not in CLP cfB$^{-/-}$ mice. Original magnification ×400. (**D**) Kidney NGAL and KIM-1 mRNA expression in WT and cfB$^{-/-}$ mice. Mice subjected to the sham and CLP procedures. Twenty-four hours later, mice were euthanized, and the kidney tissues were harvested. NGAL and KIM-1 mRNA were determined by qRT-PCR. Data were plotted as median with 10th and 90th percentile in the bottom and top, respectively, and analyzed by two-way ANOVA with Mann–Whitney nonparameter post test. $n = 4$ in sham group, $n = 6$ to 7 in CLP group. *$p < 0.05$, **$p < 0.01$. (**E**) Anti-cfB Ab mAb1379 attenuates NGAL and KIM-1 mRNA expression during sepsis. mAb1379 (1 mg) was administered i.p. 1 h before and every 12 h after CLP surgery. Kidneys were harvested at 12 and 24 h postsurgery and analyzed for NGAL and KIM-1 mRNA expression. $n = 7$ in sham group (combination of sham mice at 12 and 24 h), $n = 5$–7 in CLP group. *$p < 0.05$, **$p < 0.01$.

and robust upregulation of cfB in multiple organs. In the heart and kidney, cfB is primarily localized in cardiomyocytes and in cortical tubular cells, respectively. Unlike the in vitro studies described above, absence of TLR2, TLR4, or Trif did not attenuate cardiac cfB expression during sepsis in vivo. This is not surprising, as multiple TLRs become activated during polymicrobial sepsis, and deletion of any one type of TLRs may not be sufficient to attenuate cfB induction. However, absence of MyD88, an adaptor essential for all TLRs except TLR3, but not Trif, effectively attenuated both local (cardiac) and systemic (serum) cfB expression, suggesting that cfB induction during polymicrobial sepsis is partially MyD88 mediated. It is worth noting that in a same model of polymicrobial sepsis, absence of MyD88 but not Trif confers protection against organ injury and mortality (51, 52).

We show that polymicrobial sepsis not only upregulates cfB levels in various organs and in the serum, but also activates the AP and induces C3 cleavage, as evidenced by markedly increased Ba and C3dg fragments in serum and the peritoneal space in vivo. AP plays a critical role in initiating and amplifying the downstream C3 cleavage during the complement activation (53). In our study, zymosan or bacteria isolated from the septic animals cause robust serum AP activation in vitro that clearly requires the presence of factor D, which may indicate the essential role of factor D in the pathogen-induced AP activation during polymicrobial sepsis. Moreover, in vivo, MyD88 deletion partially blocks the bacteria-induced serum cfB expression and AP activation (reduced cfB and Ba production), demonstrating the TLR control over the AP activation during bacterial sepsis. However, it is worth noting that the lower serum cfB/C3 fragments in septic MyD88$^{-/-}$ mice is likely due to reduced total cfB/C3 in these knockout mice because the in vitro AP assay indicates that MyD88 is not involved in the zymosan/bacteria-induced AP activation per se. The fact that cfB deficiency has no impact on the overall levels of C3 in our study suggests that bacteria-induced C3 upregulation is cfB-independent. In contrast, cfB appears essential for sepsis-induced C3α cleavage as cfB$^{-/-}$ animals have markedly reduced C3dg in response to sepsis, suggesting that C3 cleavage is mainly dependent on cfB/AP during sepsis. Consistent with this is that cfB$^{-/-}$ septic mice have much less kidney C3 fragment deposition than WT septic mice, which may explain in part the attenuated tissue damage observed in cfB$^{-/-}$ septic mice. Local C3 fragment deposition has been shown to mediate (54, 55) and C3dg-targeted inhibition to reduce tissue injury (50). Complement receptor 2 (CR2) is a receptor of C3 fragments in the mouse. Inhibition by

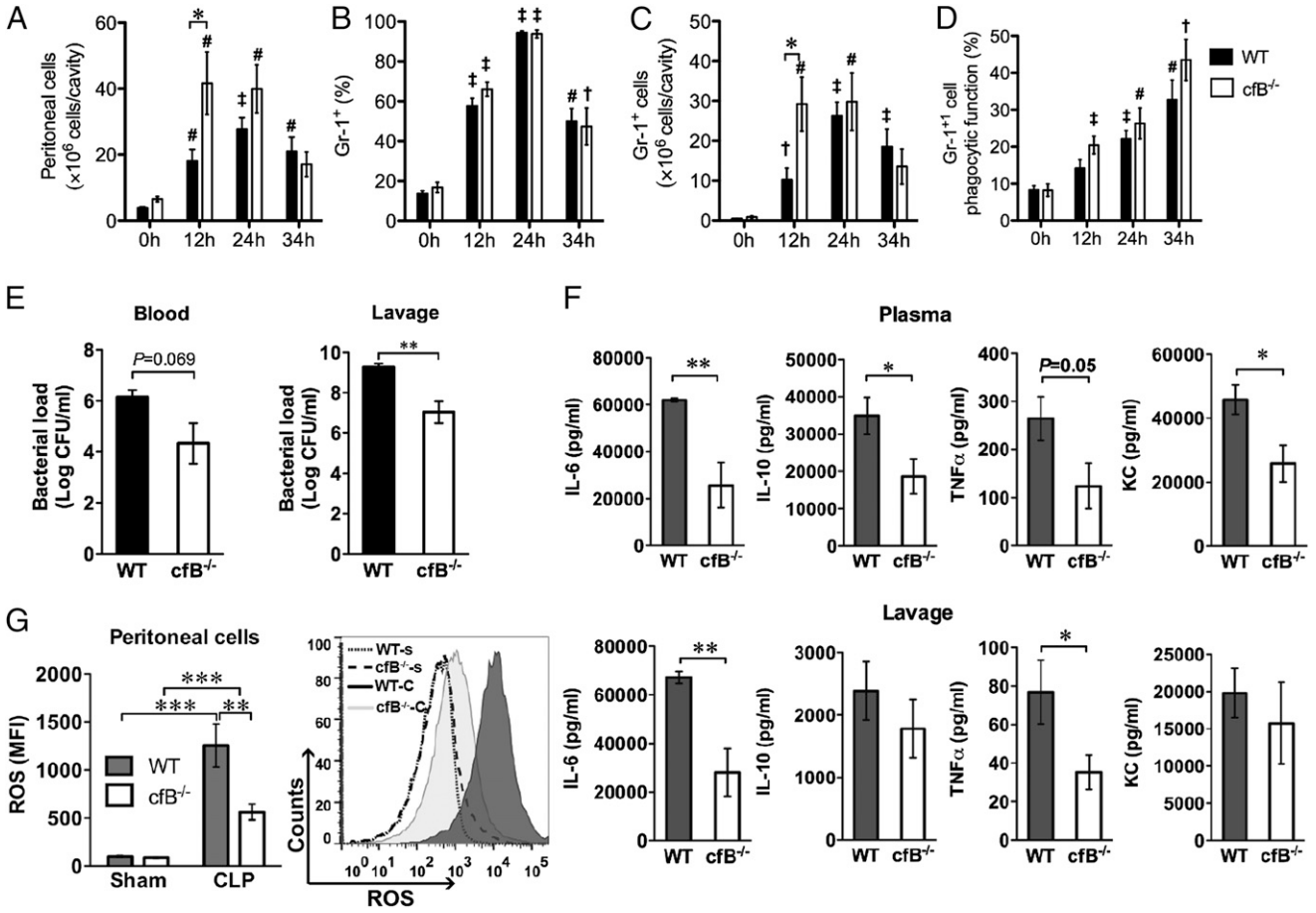

FIGURE 6. cfB deficiency leads to enhanced neutrophil migration, attenuated cytokine responses, decreased bacterial loading, and ROS generation during peritoneal sepsis. (**A**–**D**) Neutrophil migratory and phagocytic functions. Mice were subjected to CLP procedure. At 0, 12, 24, and 34 h after CLP, normal saline (5 ml) was injected into the peritoneal cavity, and the peritoneal lavage was harvested. Total peritoneal cells were counted manually, and Gr-1^+ neutrophils were determined by flow cytometer. (A) Time course of peritoneal cell accumulation following CLP. (B) Percentage of Gr-1^+ neutrophils among the peritoneal cells as measured by flow cytometry. (C) Total number of Gr-1^+ neutrophils migrated into the peritoneal space were calculated as: total peritoneal cells × percentage of Gr-1^+ cells. (D) Phagocytic neutrophils in the peritoneal cavity. Peritoneal cells were incubated with opsonized fluorescent microspheres (FITC) at 37°C for 30 min and then stained with allophycocyanin-labeled Gr-1 Ab. Percentage of phagocytic neutrophils was presented as both FITC-bead$^+$ and allophycocyanin–Gr-1^+. n = 7–9 at time 0, n = 7–14 at time 12 h, n = 6–12 at time 24 h, n = 3–7 at time 34 h. $^{\dagger}p < 0.05$, $^{\ddagger}p < 0.01$, $^{\#}p < 0.001$ versus time 0 h. $^{*}p < 0.05$ versus WT. (**E**) Bacterial counting. Bacterial loading was assessed in both blood and peritoneal lavage fluids. n = 8 to 9 in WT group, n = 10 in cfB$^{-/-}$ group. $^{**}p < 0.01$. (**F**) Cytokine production. Cytokine/chemokine levels in the plasma and peritoneal lavage were measured by Luminex multiplex assays. n = 8 to 9 in WT group, n = 10 in cfB$^{-/-}$ group. $^{*}p < 0.05$, $^{**}p < 0.01$. (**G**) ROS production in peritoneal neutrophils. Twelve hours after sham or CLP surgery, the peritoneal cells were collected, incubated with 10 μM DCF, and analyzed for intracellular ROS production by flow cytometry. n = 11 in sham group, n = 21 in CLP group. A representative histogram is in the right column. $^{*}p < 0.05$, $^{**}p < 0.01$, $^{***}p < 0.001$. cfB$^{-/-}$-C, cfB$^{-/-}$-CLP; cfB$^{-/-}$-s, cfB$^{-/-}$-sham; MFI, mean fluorescence intensity; WT-C, WT-CLP; WT-s, WT-sham.

CR2–factor H (blocking AP at C3 activation) provides more effective protection than CR2-Crry (blocking all pathways at C3 activation) in an acute murine colitis model, suggesting that AP plays a key role in tissue inflammation and injury and that the classical/lectin pathway provides important protection in host defense (55). Finally, supporting the role of cfB/AP in sepsis is a recent study in which patients with severe sepsis admitted to emergency departments had extensive complement activation, particularly of the AP (23).

The complement system represents a rapid and efficient immune surveillance system that acts against foreign pathogens (7). In a nonsevere model of polymicrobial peritonitis, mice deficient in C1q (lack classical pathway) or deficient in cfB and C2 (lack all three pathways) have an increased mortality rate compared with WT mice, indicating a critical contribution of the three complement pathways to host defense (56). However, under severe septic and hyperinflammatory conditions, they may be improperly controlled and may contribute to tissue injury and organ failure (57). One example is C5a (57). Blockade of C5a confers a survival benefit in a CLP model of sepsis (58) and improved multiple organ functions (59). Our study provides yet another mechanism by which the complement system contributes to the pathogenesis of sepsis. Animals lacking cfB have a significantly improved survival, better preserved cardiac function, and reduced kidney injury. During sepsis cfB is markedly upregulated in the major organs including the heart and kidney. Tissue-deposited cfB fragments likely induce organ injury through the AP-mediated C3 cleavage and deposition, although a direct injurious effect by cfB on these organs cannot be ruled out. Recent studies have shown that cfB appears to have a property of inducing cell membrane injury and activating apoptosis program. For instance, cfB contributes to endotoxin-triggered sarcolemmal injury (16). Renal ischemia/reperfusion-induced caspase activation is cfB dependent (17), although in our study cfB deficiency had no impact on sepsis-induced caspase-3 activation in the spleen. Finally, given its contributory role in sepsis, reduced C5a in cfB$^{-/-}$ mice might

explain the improved outcome in these mice. However, this seems less likely because C5a is effectively generated, both at the baseline and during sepsis, in the absence of AP in factor D–deficient mice (60).

Several factors may contribute to the survival benefit in septic cfB$^{-/-}$ mice. These include enhanced early neutrophil migration to the infectious site, attenuated cytokine storm locally and systemically, reduced ROS generation in neutrophils isolated from septic mice, and decreased bacterial load. These data suggest that absence of cfB and AP activation does not seem to comprise the host's ability to clear bacteria during polymicrobial sepsis, but rather enhances some elements of the innate immunity such as neutrophil migratory function and attenuates injurious mechanisms such as neutrophil ROS production and tissue C3 fragment deposition. Somewhat different from the current study, a recent report demonstrated that deficiency of factor D does not significantly impact on animal survival in a similar model of polymicrobial sepsis (60). Cleavage of cfB by cfD is considered the key step in the formation of the convertase C3bBb (61). Similar to cfB$^{-/-}$ mice in the current study, cfD$^{-/-}$ mice exhibit reduction in tissue C3 deposition and increased neutrophil recruitment (60). However, cfD$^{-/-}$ mice display organ dysfunction and bacterial load at the level similar to WT mice and systemic cytokine responses higher than WT mice (60). In contrast, C1q$^{-/-}$ mice have significantly higher bacterial load than WT and cfD$^{-/-}$ mice (60), suggesting a predominant role of the classical pathway in host bacterial clearance. However, it is worth noting that whereas cfB cleavage is totally prevented in cfD$^{-/-}$ animals, AP activation in cfD$^{-/-}$ mice still exists after cobra venom factor (a functional C3b analog and AP activator) administration. Both cobra venom factor–dependent C3 consumption in vivo and C3 α-chain cleavage in vitro remain largely intact, albeit at a significantly slower rate (61). Thus, the possible AP activation in the cfD$^{-/-}$ mice might explain the indifference of bacterial loading and survival outcome in these animals compared with WT. Taken together, our study indicates that specific deletion or inhibition of cfB reduces tissue injury and improves survival without compromising host defense against invading bacteria.

In summary, the current study demonstrates that cfB is a downstream effector of TLRs and contributes to the pathogenesis of severe sepsis. TLR activation in vitro and polymicrobial sepsis in vivo specifically induces de novo cfB production in distinct cell types such as macrophages and cardiomyocytes and in major organs such as the kidney. Signaling via MyD88 mediates cfB/C3 upregulation and contributes to AP activation during polymicrobial sepsis. Lack of cfB markedly reduces C3 cleavage and kidney deposition of C3 fragments and confers a survival benefit in septic mice. Our results suggest cfB plays a major role in mediating cardiac dysfunction, AKI, and mortality during polymicrobial peritonitis sepsis, which is in part related to a reduction in ROS production and systemic inflammation.

Acknowledgments

We thank Yan Liu, Shenjun Zhu, Junlei Chang, and Kentaro Tokuda of Massachusetts General Hospital for technical support.

Disclosures

The authors have no financial conflicts of interest.

References

1. Bone, R. C., R. A. Balk, F. B. Cerra, R. P. Dellinger, A. M. Fein, W. A. Knaus, R. M. Schein, and W. J. Sibbald. 1992. Definitions for sepsis and organ failure and guidelines for the use of innovative therapies in sepsis. The ACCP/SCCM Consensus Conference Committee. American College of Chest Physicians/Society of Critical Care Medicine. *Chest* 101: 1644–1655.
2. Dombrovskiy, V. Y., A. A. Martin, J. Sunderram, and H. L. Paz. 2007. Rapid increase in hospitalization and mortality rates for severe sepsis in the United States: a trend analysis from 1993 to 2003. *Crit. Care Med.* 35: 1244–1250.
3. Parrillo, J. E. 2008. Septic shock–vasopressin, norepinephrine, and urgency. *N. Engl. J. Med.* 358: 954–956.
4. Angus, D. C., W. T. Linde-Zwirble, J. Lidicker, G. Clermont, J. Carcillo, and M. R. Pinsky. 2001. Epidemiology of severe sepsis in the United States: analysis of incidence, outcome, and associated costs of care. *Crit. Care Med.* 29: 1303–1310.
5. Medzhitov, R. 2007. Recognition of microorganisms and activation of the immune response. *Nature* 449: 819–826.
6. Markiewski, M. M., and J. D. Lambris. 2007. The role of complement in inflammatory diseases from behind the scenes into the spotlight. *Am. J. Pathol.* 171: 715–727.
7. Ricklin, D., G. Hajishengallis, K. Yang, and J. D. Lambris. 2010. Complement: a key system for immune surveillance and homeostasis. *Nat. Immunol.* 11: 785–797.
8. Medzhitov, R., and C. Janeway, Jr. 2000. The Toll receptor family and microbial recognition. *Trends Microbiol.* 8: 452–456.
9. Alves-Filho, J. C., A. Freitas, F. O. Souto, F. Spiller, H. Paula-Neto, J. S. Silva, R. T. Gazzinelli, M. M. Teixeira, S. H. Ferreira, and F. Q. Cunha. 2009. Regulation of chemokine receptor by Toll-like receptor 2 is critical to neutrophil migration and resistance to polymicrobial sepsis. *Proc. Natl. Acad. Sci. USA* 106: 4018–4023.
10. Zou, L., Y. Feng, Y. J. Chen, R. Si, S. Shen, Q. Zhou, F. Ichinose, M. Scherrer-Crosbie, and W. Chao. 2010. Toll-like receptor 2 plays a critical role in cardiac dysfunction during polymicrobial sepsis. *Crit. Care Med.* 38: 1335–1342.
11. Cavassani, K. A., M. Ishii, H. Wen, M. A. Schaller, P. M. Lincoln, N. W. Lukacs, C. M. Hogaboam, and S. L. Kunkel. 2008. TLR3 is an endogenous sensor of tissue necrosis during acute inflammatory events. *J. Exp. Med.* 205: 2609–2621.
12. Alves-Filho, J. C., A. de Freitas, M. Russo, and F. Q. Cunha. 2006. Toll-like receptor 4 signaling leads to neutrophil migration impairment in polymicrobial sepsis. *Crit. Care Med.* 34: 461–470.
13. Roger, T., C. Froidevaux, D. Le Roy, M. K. Reymond, A. L. Chanson, D. Mauri, K. Burns, B. M. Riederer, S. Akira, and T. Calandra. 2009. Protection from lethal gram-negative bacterial sepsis by targeting Toll-like receptor 4. *Proc. Natl. Acad. Sci. USA* 106: 2348–2352.
14. Plitas, G., B. M. Burt, H. M. Nguyen, Z. M. Bamboat, and R. P. DeMatteo. 2008. Toll-like receptor 9 inhibition reduces mortality in polymicrobial sepsis. *J. Exp. Med.* 205: 1277–1283.
15. Matsumoto, M., W. Fukuda, A. Circolo, J. Goellner, J. Strauss-Schoenberger, X. Wang, S. Fujita, T. Hidvegi, D. D. Chaplin, and H. R. Colten. 1997. Abrogation of the alternative complement pathway by targeted deletion of murine factor B. *Proc. Natl. Acad. Sci. USA* 94: 8720–8725.
16. Singh, M. V., A. Kapoun, L. Higgins, W. Kutschke, J. M. Thurman, R. Zhang, M. Singh, J. Yang, X. Guan, J. S. Lowe, et al. 2009. Ca2+/calmodulin-dependent kinase II triggers cell membrane injury by inducing complement factor B gene expression in the mouse heart. *J. Clin. Invest.* 119: 986–996.
17. Thurman, J. M., P. A. Royer, D. Ljubanovic, B. Dursun, A. M. Lenderink, C. L. Edelstein, and V. M. Holers. 2006. Treatment with an inhibitory monoclonal antibody to mouse factor B protects mice from induction of apoptosis and renal ischemia/reperfusion injury. *J. Am. Soc. Nephrol.* 17: 707–715.
18. Zhang, X., Y. Kimura, C. Fang, L. Zhou, G. Sfyroera, J. D. Lambris, R. A. Wetsel, T. Miwa, and W. C. Song. 2007. Regulation of Toll-like receptor-mediated inflammatory response by complement in vivo. *Blood* 110: 228–236.
19. Fang, C., X. Zhang, T. Miwa, and W. C. Song. 2009. Complement promotes the development of inflammatory T-helper 17 cells through synergistic interaction with Toll-like receptor signaling and interleukin-6 production. *Blood* 114: 1005–1015.
20. Kaczorowski, D. J., A. Afrazi, M. J. Scott, J. H. Kwak, R. Gill, R. D. Edmonds, Y. Liu, J. Fan, and T. R. Billiar. 2010. Pivotal advance: The pattern recognition receptor ligands lipopolysaccharide and polyinosine-polycytidylic acid stimulate factor B synthesis by the macrophage through distinct but overlapping mechanisms. *J. Leukoc. Biol.* 88: 609–618.
21. Hajishengallis, G., and J. D. Lambris. 2010. Crosstalk pathways between Toll-like receptors and the complement system. *Trends Immunol.* 31: 154–163.
22. Goring, K., Y. Huang, C. Mowat, C. Leger, T. H. Lim, R. Zaheer, D. Mok, L. A. Tibbles, D. Zygun, and B. W. Winston. 2009. Mechanisms of human complement factor B induction in sepsis and inhibition by activated protein C. *Am. J. Physiol. Cell Physiol.* 296: C1140–C1150.
23. Younger, J. G., D. O. Bracho, H. M. Chung-Esaki, M. Lee, G. K. Rana, A. Sen, and A. E. Jones. 2010. Complement activation in emergency department patients with severe sepsis. *Acad. Emerg. Med.* 17: 353–359.
24. Takeuchi, O., K. Hoshino, T. Kawai, H. Sanjo, H. Takada, T. Ogawa, K. Takeda, and S. Akira. 1999. Differential roles of TLR2 and TLR4 in recognition of gram-negative and gram-positive bacterial cell wall components. *Immunity* 11: 443–451.
25. Yamamoto, M., S. Sato, H. Hemmi, K. Hoshino, T. Kaisho, H. Sanjo, O. Takeuchi, M. Sugiyama, M. Okabe, K. Takeda, and S. Akira. 2003. Role of adaptor TRIF in the MyD88-independent toll-like receptor signaling pathway. *Science* 301: 640–643.
26. Kawai, T., O. Adachi, T. Ogawa, K. Takeda, and S. Akira. 1999. Unresponsiveness of MyD88-deficient mice to endotoxin. *Immunity* 11: 115–122.
27. Li, Y., R. Si, Y. Feng, H. H. Chen, L. Zou, E. Wang, M. Zhang, H. S. Warren, D. E. Sosnovik, and W. Chao. 2011. Myocardial ischemia activates an injurious

innate immune signaling via cardiac heat shock protein 60 and Toll-like receptor 4. *J. Biol. Chem.* 286: 31308–31319.
28. Zou, L., Y. Feng, M. Zhang, Y. Li, and W. Chao. 2011. Nonhematopoietic toll-like receptor 2 contributes to neutrophil and cardiac function impairment during polymicrobial sepsis. *Shock* 36: 370–380.
29. Rittirsch, D., M. S. Huber-Lang, M. A. Flierl, and P. A. Ward. 2009. Immunodesign of experimental sepsis by cecal ligation and puncture. *Nat. Protoc.* 4: 31–36.
30. Thurman, J. M., D. M. Kraus, G. Girardi, D. Hourcade, H. J. Kang, P. A. Royer, L. M. Mitchell, P. C. Giclas, J. Salmon, G. Gilkeson, and V. M. Holers. 2005. A novel inhibitor of the alternative complement pathway prevents antiphospholipid antibody-induced pregnancy loss in mice. *Mol. Immunol.* 42: 87–97.
31. Leinhase, I., M. Rozanski, D. Harhausen, J. M. Thurman, O. I. Schmidt, A. M. Hossini, M. E. Taha, D. Rittirsch, P. A. Ward, V. M. Holers, et al. 2007. Inhibition of the alternative complement activation pathway in traumatic brain injury by a monoclonal anti-factor B antibody: a randomized placebo-controlled study in mice. *J. Neuroinflammation* 4: 13.
32. Quigg, R. J., Y. Kozono, D. Berthiaume, A. Lim, D. J. Salant, A. Weinfeld, P. Griffin, E. Kremmer, and V. M. Holers. 1998. Blockade of antibody-induced glomerulonephritis with Crry-Ig, a soluble murine complement inhibitor. *J. Immunol.* 160: 4553–4560.
33. Morgan, B. P., and P. Gasque. 1997. Extrahepatic complement biosynthesis: where, when and why? *Clin. Exp. Immunol.* 107: 1–7.
34. Farrar, C. A., W. Zhou, T. Lin, and S. H. Sacks. 2006. Local extravascular pool of C3 is a determinant of postischemic acute renal failure. *FASEB J.* 20: 217–226.
35. Vieyra, M. B., and P. S. Heeger. 2010. Novel aspects of complement in kidney injury. *Kidney Int.* 77: 495–499.
36. Verschoor, A., M. A. Brockman, M. Gadjeva, D. M. Knipe, and M. C. Carroll. 2003. Myeloid C3 determines induction of humoral responses to peripheral herpes simplex virus infection. *J. Immunol.* 171: 5363–5371.
37. Lambris, J. D., Z. Lao, T. J. Oglesby, J. P. Atkinson, C. E. Hack, and J. D. Becherer. 1996. Dissection of CR1, factor H, membrane cofactor protein, and factor B binding and functional sites in the third complement component. *J. Immunol.* 156: 4821–4832.
38. Uchino, S., J. A. Kellum, R. Bellomo, G. S. Doig, H. Morimatsu, S. Morgera, M. Schetz, I. Tan, C. Bouman, E. Macedo, et al. 2005. Acute renal failure in critically ill patients: a multinational, multicenter study. *JAMA* 294: 813–818.
39. Doi, K., A. Leelahavanichkul, P. S. Yuen, and R. A. Star. 2009. Animal models of sepsis and sepsis-induced kidney injury. *J. Clin. Invest.* 119: 2868–2878.
40. Zarjou, A., and A. Agarwal. 2011. Sepsis and acute kidney injury. *J. Am. Soc. Nephrol.* 22: 999–1006.
41. Zhang, Z., B. D. Humphreys, and J. V. Bonventre. 2007. Shedding of the urinary biomarker kidney injury molecule-1 (KIM-1) is regulated by MAP kinases and juxtamembrane region. *J. Am. Soc. Nephrol.* 18: 2704–2714.
42. Siew, E. D., L. B. Ware, T. Gebretsadik, A. Shintani, K. G. Moons, N. Wickersham, F. Bossert, and T. A. Ikizler. 2009. Urine neutrophil gelatinase-associated lipocalin moderately predicts acute kidney injury in critically ill adults. *J. Am. Soc. Nephrol.* 20: 1823–1832.
43. Paragas, N., A. Qiu, Q. Zhang, B. Samstein, S. X. Deng, K. M. Schmidt-Ott, M. Viltard, W. Yu, C. S. Forster, G. Gong, et al. 2011. The Ngal reporter mouse detects the response of the kidney to injury in real time. *Nat. Med.* 17: 216–222.
44. Devarajan, P. 2010. Review: neutrophil gelatinase-associated lipocalin: a troponin-like biomarker for human acute kidney injury. *Nephrology (Carlton)* 15: 419–428.
45. Bosmann, M., and P. A. Ward. 2013. The inflammatory response in sepsis. *Trends Immunol.* 34: 129–136.
46. Hotchkiss, R. S., K. C. Chang, P. E. Swanson, K. W. Tinsley, J. J. Hui, P. Klender, S. Xanthoudakis, S. Roy, C. Black, E. Grimm, et al. 2000. Caspase inhibitors improve survival in sepsis: a critical role of the lymphocyte. *Nat. Immunol.* 1: 496–501.
47. Naik, E., and V. M. Dixit. 2011. Mitochondrial reactive oxygen species drive proinflammatory cytokine production. *J. Exp. Med.* 208: 417–420.
48. Crimi, E., V. Sica, A. S. Slutsky, H. Zhang, S. Williams-Ignarro, L. J. Ignarro, and C. Napoli. 2006. Role of oxidative stress in experimental sepsis and multisystem organ dysfunction. *Free Radic. Res.* 40: 665–672.
49. Bayir, H. 2005. Reactive oxygen species. *Crit. Care Med.* 33: S498–S501.
50. Atkinson, C., H. Song, B. Lu, F. Qiao, T. A. Burns, V. M. Holers, G. C. Tsokos, and S. Tomlinson. 2005. Targeted complement inhibition by C3d recognition ameliorates tissue injury without apparent increase in susceptibility to infection. *J. Clin. Invest.* 115: 2444–2453.
51. Weighardt, H., S. Kaiser-Moore, R. M. Vabulas, C. J. Kirschning, H. Wagner, and B. Holzmann. 2002. Cutting edge: myeloid differentiation factor 88 deficiency improves resistance against sepsis caused by polymicrobial infection. *J. Immunol.* 169: 2823–2827.
52. Feng, Y., L. Zou, M. Zhang, Y. Li, C. Chen, and W. Chao. 2011. MyD88 and Trif signaling play distinct roles in cardiac dysfunction and mortality during endotoxin shock and polymicrobial sepsis. *Anesthesiology* 115: 555–567.
53. Harboe, M., and T. E. Mollnes. 2008. The alternative complement pathway revisited. *J. Cell. Mol. Med.* 12: 1074–1084.
54. Sheerin, N. S., P. Risley, K. Abe, Z. Tang, W. Wong, T. Lin, and S. H. Sacks. 2008. Synthesis of complement protein C3 in the kidney is an important mediator of local tissue injury. *FASEB J.* 22: 1065–1072.
55. Schepp-Berglind, J., C. Atkinson, M. Elvington, F. Qiao, P. Mannon, and S. Tomlinson. 2012. Complement-dependent injury and protection in a murine model of acute dextran sulfate sodium-induced colitis. *J. Immunol.* 188: 6309–6318.
56. Windbichler, M., B. Echtenacher, T. Hehlgans, J. C. Jensenius, W. Schwaeble, and D. N. Mannel. 2004. Involvement of the lectin pathway of complement activation in antimicrobial immune defense during experimental septic peritonitis. *Infect. Immun.* 72: 5247–5252.
57. Ward, P. A. 2004. The dark side of C5a in sepsis. *Nat. Rev. Immunol.* 4: 133–142.
58. Czermak, B. J., V. Sarma, C. L. Pierson, R. L. Warner, M. Huber-Lang, N. M. Bless, H. Schmal, H. P. Friedl, and P. A. Ward. 1999. Protective effects of C5a blockade in sepsis. *Nat. Med.* 5: 788–792.
59. Huber-Lang, M., V. J. Sarma, K. T. Lu, S. R. McGuire, V. A. Padgaonkar, R. F. Guo, E. M. Younkin, R. G. Kunkel, J. Ding, R. Erickson, et al. 2001. Role of C5a in multiorgan failure during sepsis. *J. Immunol.* 166: 1193–1199.
60. Dahlke, K., C. D. Wrann, O. Sommerfeld, M. Sossdorf, P. Recknagel, S. Sachse, S. W. Winter, A. Klos, G. L. Stahl, Y. X. Ma, et al. 2011. Distinct different contributions of the alternative and classical complement activation pathway for the innate host response during sepsis. *J. Immunol.* 186: 3066–3075.
61. Xu, Y., M. Ma, G. C. Ippolito, H. W. Schroeder, Jr., M. C. Carroll, and J. E. Volanakis. 2001. Complement activation in factor D-deficient mice. *Proc. Natl. Acad. Sci. USA* 98: 14577–14582.